Experimental observation of the triplet spin-valve effect in a superconductor-ferromagnet heterostructure

V. I. Zdravkov,[1,2] J. Kehrle,[1] G. Obermeier,[1] D. Lenk,[1] H.-A. Krug von Nidda,[1] C. Müller,[1] M. Yu. Kupriyanov,[3] A. S. Sidorenko,[2] S. Horn,[1] R. Tidecks,[1] and L. R. Tagirov[1,4]
[1]*Institut für Physik, Universität Augsburg, D-86159 Augsburg, Germany*
[2]*Institute of Electronic Engineering and Nanotechnologies ASM, Kishinev MD-2028, Moldova*
[3]*Skobeltsyn Institute of Nuclear Physics, Moscow State University, Moscow 119992, Russia*
[4]*Solid State Physics Department, Kazan Federal University, 420008 Kazan, Russia*
(Received 1 March 2012; revised manuscript received 9 February 2013; published 12 April 2013)

The theory of superconductor-ferromagnet heterostructures with two ferromagnetic layers predicts the generation of a long-range, odd-in-frequency triplet pairing at noncollinear alignment (NCA) of the magnetizations of the F layers. This triplet pairing has been detected in a Nb/$Cu_{41}Ni_{59}$/normal conducting- (nc-) Nb/Co/CoO_x spin-valve-type proximity effect heterostructure, in which a very thin Nb film between the F layers serves as a spacer of nc metal. The resistance of the sample as a function of an external magnetic field shows that for not too high fields, the system is superconducting at a collinear alignment of the $Cu_{41}Ni_{59}$ and Co layer magnetic moments but switches to the normal conducting state at a NCA configuration. This indicates that the superconducting transition temperature T_c for NCA is lower than the fixed measuring temperature. The existence of a minimum T_c, at the NCA regime below that one for parallel or antiparallel alignments of the F-layer magnetic moments, is consistent with the theoretical prediction of a singlet superconductivity suppression by the long-range triplet pairing generation.

DOI: 10.1103/PhysRevB.87.144507 PACS number(s): 74.45.+c, 74.81.−g, 85.25.Am

I. INTRODUCTION

An odd-in-frequency triplet pairing generation in singlet superconductor/ferromagnet thin-film heterostructures was predicted theoretically.[1–3] At least two ferromagnetic layers (F_1,F_2) with a noncollinear alignment (NCA) of their magnetizations are required to couple the conventional opposite-spin singlet s-wave pairing channel with the unconventional, odd-triplet s-wave pairing channel. The latter one is of extraordinary long range in F layers,[1,2,4] because the magnetized conduction band of a ferromagnetic metal serves as an eigenmedia supporting the equal-spin pairing.

Intense activities followed to formulate optimal conditions and to realize experimental schemes for generation and detection of this odd-triplet pairing using the Josephson effect.[5–14] The observation of a current crossing a weak link of ferromagnetic material with a thickness much exceeding the penetration length for singlet-paired electrons[5–11] indicated a triplet contribution to the Josephson current.

In superconductor-ferromagnet proximity-type experiments, also the odd-triplet pairing was considered.[15,16] In a recent paper,[17] a deep absolute minimum of the superconducting (SC) transition temperature, T_c, due to the odd-triplet component generation was predicted for a S/F_1/F_2 SC spin-valve heterostructure near the crossed (CR) configuration of the magnetic moments of the adjacent F_1 and F_2 layers. The aim of the present work is to realize this odd-triplet pairing induced spin-valve effect experimentally.

An S/F_1/N/F_2/AF spin-valve heterostructure (Fig. 1) was used. Here, S is a singlet superconductor (Nb), F_1 and F_2 are metallic ferromagnet layers ($Cu_{41}Ni_{59}$ alloy and Co), N is a spacer of normal conducting (nc) metal (very thin Nb, below the critical thickness[18,19]), and AF denotes an insulating antiferromagnet (CoO_x), to exchange bias the magnetic moment of the F_2 layer.

The equilibrium magnetization of the $Cu_{41}Ni_{59}$ alloy is perpendicular to the layer plane.[20,21] For thin Co films, an exchange bias induces an in-plane unidirectional anisotropy so that the magnetization lies in the film plane.[22] Then, with an external magnetic field applied parallel to the plane of the heterostructure, one could control the magnetic configuration of the system from a parallel alignment (PA) through a CR one toward an antiparallel alignment (APA) of the F-layer magnetic moments (see the sketch in Fig. 1 and measurements below).

II. SAMPLE PREPARATION AND CHARACTERIZATION

The thin film samples were deposited by magnetron sputtering on commercial (111) silicon substrates at 300 K. In the Leybold Z400 vacuum system, the base pressure was about 2×10^{-6} mbar. Pure argon (99.999%) with 8×10^{-3} mbar served as sputter gas. To obtain samples with different thicknesses of the $Cu_{41}Ni_{59}$ alloy, a wedge-shaped layer was deposited by rf magnetron sputtering as described in Refs. 18 and 19. To get a smooth Nb layer of constant thickness and to control precisely the film growth rate, we moved the target during the dc sputtering process of the Nb layer (spray technology[18,19]). The average growth rate of the Nb film was about 1.3 nm/sec, while the rate of the sputtering process was adjusted to 4 nm/sec, to reduce the amount of contaminations gettered in the Nb film. The metallic Co layer was deposited by rf sputtering. Reactive oxygen gas was mixed to argon to deposit a CoO_x oxide layer. The resulting specimen, Nb/$Cu_{41}Ni_{59}$-wedge/nc-Nb/Co/CoO_x, was sequentially cut perpendicular to the CuNi thickness gradient on 25 stripes of typical size 2.5×8 mm^2 and numbered from #1 to #25, starting from the thick side. A series of Nb/$Cu_{41}Ni_{59}$/Si-cap pilot S/F_1 bilayers for magnetoresistance (MR) measurements

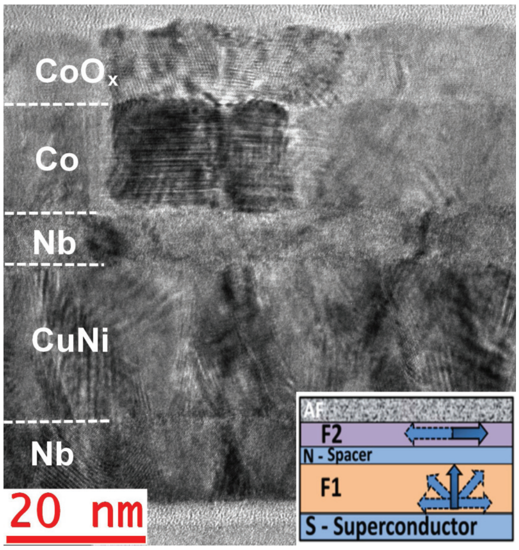

FIG. 1. (Color) The $Nb/Cu_{41}Ni_{59}/nc\text{-}Nb/Co/CoO_x$ sample cross section. TEM image of sample SF_1NF_2-AF1 #5. Arrows in the sketch indicate possible directions of the layers magnetic moments. The thicknesses of the layers for sample #5 obtained from the TEM image are about 12, 23, 7, 16, and 11.5 nm for Nb, CuNi, Nb-spacer, Co, and CoO_x respectively, whereas for sample #20 (not shown here), they are about 12, 6.5, 6, 22 and 14.5 nm.

and a four-wedge $(Cu_{41}Ni_{59}\text{-wedge/Si}) \times 4$ sample reference series for magnetic measurements were fabricated by the same technique. The thicknesses of the different layers of the samples, for which hysteresis and MR measurements are presented below, were determined by Rutherford backscattering spectrometry,[18,19] considering in the case of the SF_1NF_2-AF1 series in addition cross-sectional transmission electron microscope (TEM) images of sample #5 shown in Fig. 1 and #20 not shown here.

III. RESULTS AND DISCUSSION

We first measured hysteresis loops of the reference $(Cu_{41}Ni_{59}/Si) \times 4$ samples in directions perpendicular to the sample plane and then, in-plane, parallel and perpendicular to the initial CuNi layer gradient [inset in Fig. 2(b)] using a SC quantum interference device (SQUID) magnetometer. The out-of-plane hysteresis loop (red) clearly shows easy-axis behavior [larger coercitivity and squareness compared to the in-plane loops (blue and black)]. The in-plane semieasy axis was determined as CR to the wedge gradient direction.

The desired sequence of magnetic configurations in the spin-valve heterostucture was passed applying a magnetic field along the in-plane semieasy axis of the $Cu_{41}Ni_{59}$ layer, which was simultaneously the easy axis of the Co film. The samples were cooled at a field of 10 kOe, then the magnetic hysteresis loops were recorded by a SQUID magnetometer in the field range ± 4 kOe. Results of samples SF_1NF_2-AF1#1 and #16 (adjacent to that one used for MR measurements) are shown in Fig. 2(a) and the inset, respectively.

For sample #1 (thickest $Cu_{41}Ni_{59}$ alloy layer) the $Cu_{41}Ni_{59}$ and Co layer signal could be separated according to Ref. 23 [Fig. 2(b)], which shows a clear exchange bias of

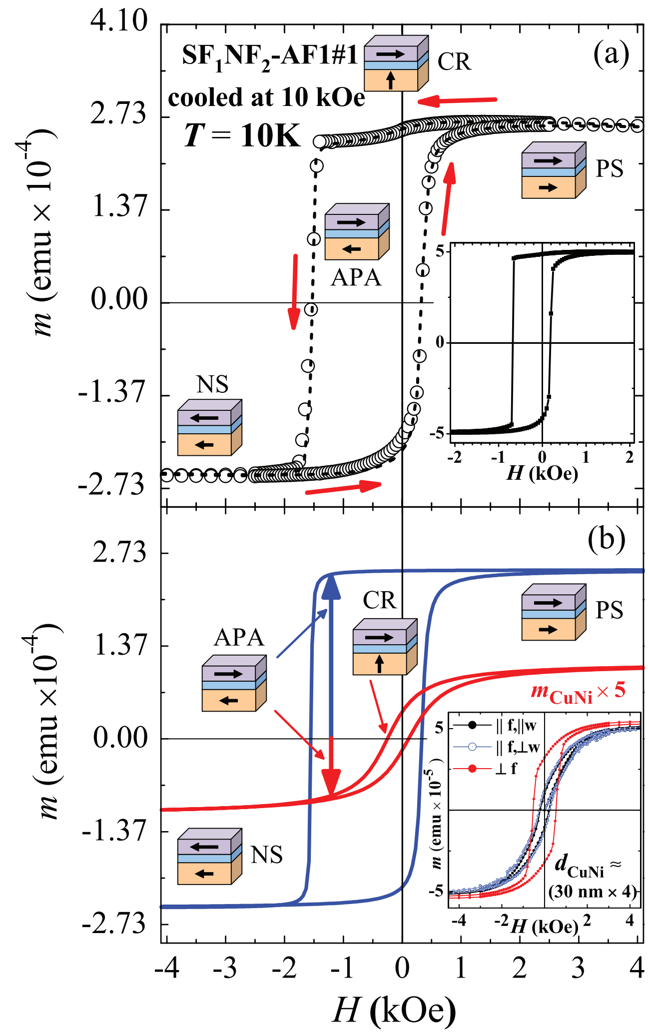

FIG. 2. (Color) (a) The magnetic moment, m, hysteresis loop (sweep route indicated) of a $Nb/Cu_{41}Ni_{59}/nc\text{-}Nb/Co/CoO_x$ specimen, sample SF_1NF_2-AF1#1 ($d_{CuNi} \approx 28$ nm). The dashed line is a modeling according to Ref. 23. Inset: hysteresis loop of SF_1NF_2-AF1#16 ($d_{CuNi} \approx 11$ nm) adjacent to the sample used for the MR measurements below. (b) Modeled components of the hysteresis loop: the blue line represents the cobalt layer and the red one the $Cu_{41}Ni_{59}$ (magnified by a factor of five). Diamagnetic contribution of the Si substrate is subtracted. Inset: hysteresis loops of the reference $(Cu_{41}Ni_{59}/Si) \times 4$ sample ($d_{CuNi} \approx 30$ nm), measured at $T = 2$ K perpendicular to the film (red $\perp$f), in the sample plane perpendicular (blue $\|$f,$\perp$w) and parallel (black $\|$f,$\|$w) to the CuNi layer thickness gradient of the wedge (see above). Pictogram abbreviations introduced in the text.

$H_{bias} \approx 940$ Oe due to the antiferromagnetic CoO_x. Resulting magnetic configurations are indicated by pictograms. Upon sweeping the field from the positive saturated (PS) configuration at +4 kOe toward the negative saturated (NS) configuration (from -1.55 to -4 kOe), the sample passes through the state with CR magnetic moments at approximately -250 Oe and the APA of the Co and $Cu_{41}Ni_{59}$ magnetic moments in the range from -250 to -1500 Oe. A similar sequence follows when sweeping the field in the reverse direction. The pilot S/F_1 bilayers behave similar to the $Cu_{41}Ni_{59}$ layer shown in red in Fig. 2(b).

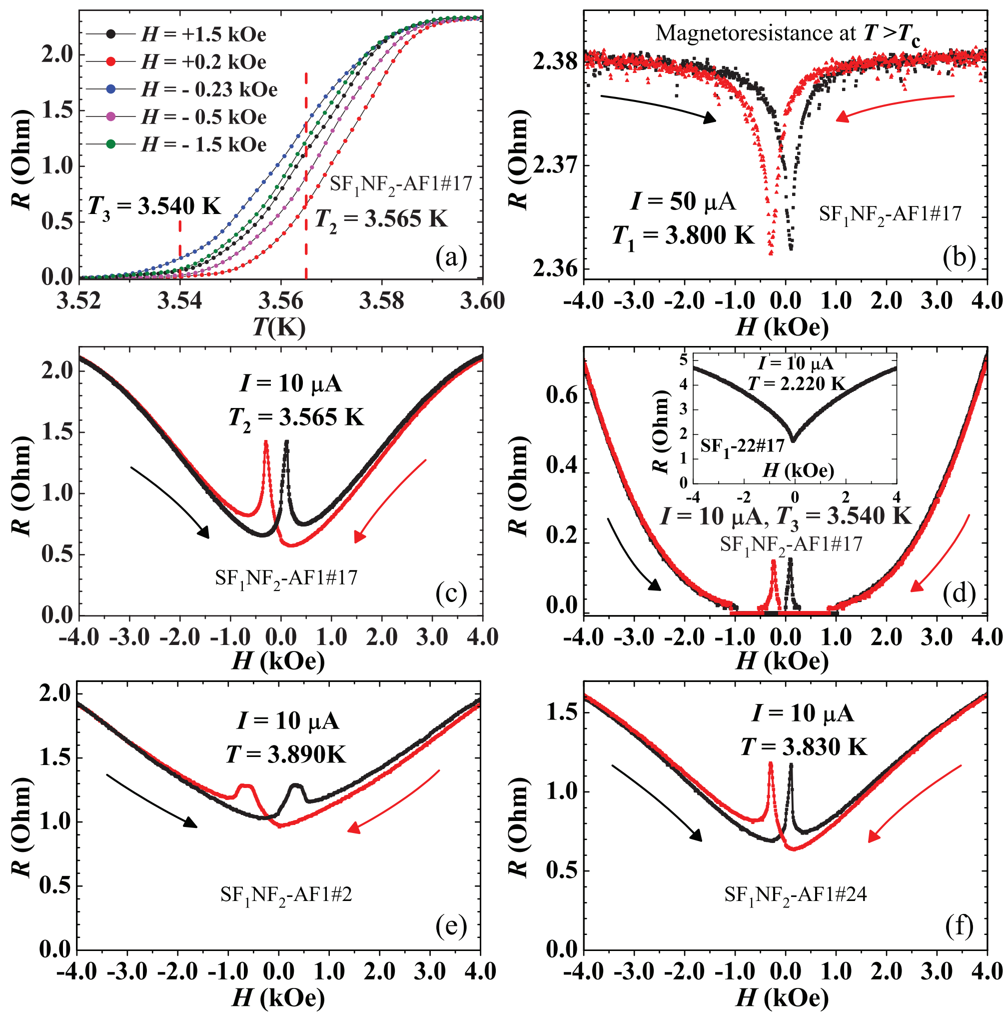

FIG. 3. (Color) Experimental results for a Nb/$Cu_{41}Ni_{59}$/nc-Nb/Co/CoO_x spin-valve structure (SF_1NF_2-AF1 series, $d_{Nb} \approx 12$ nm) measured after cooling down in a field of 30 kOe. (a) SC transition curves at different magnetic fields, sample #17, $d_{CuNi} \approx 9.5$ nm; (b) MR data recorded well above the SC transition, sample #17; (c) MR curves recorded at $T_2 \approx 3.565$ K, sample #17; (d) MR curves recorded at $T_3 \approx 3.540$ K, sample #17. Inset: MR of the pilot Nb/$Cu_{41}Ni_{59}$/Si-cap bilayer (sample SF_1-22#17, on a Si buffer layer; one has $d_{Nb} \approx 8$ nm and $d_{CuNi} \approx 16$ nm) measured in the same geometry and sequence as basic sample #17; (e) MR curves of sample #2, $d_{CuNi} \approx 27$ nm; (f) MR curves of sample #24, $d_{CuNi} \approx 1.8$ nm.

Resistance measurements were performed using the standard dc four-probe method with sensing current 10 μA (polarity alternated to eliminate thermoelectric voltages), flowing parallel to the magnetic field. Prior to the measurements, the samples were cooled at 30 kOe in a field applied parallel to the in-plane semieasy axis of the $Cu_{41}Ni_{59}$ layer as in the magnetic measurements. A set of resistance-temperature, $R(T)$, curves recorded at different magnetic fields H in this direction are given in Fig. 3(a).

The MR measurements at $T_1 \approx 3.80$ K, well above the onset of the SC transition at zero field (midpoint $T_c = 3.566$ K), are shown in Fig. 3(b). Weak downward peaks coincide with the $Cu_{41}Ni_{59}$ layer coercive fields. These results are consistent with an intrinsic magnetization of the $Cu_{41}Ni_{59}$ layer perpendicular, and that one of the Co layer parallel, to the film plane and to the current, if we assume that the anisotropic magnetoresistance (AMR) of the $Cu_{41}Ni_{59}$ layer is observed in these experiments.

The $R(H)$ measurements in the temperature range of the SC transition for sample SF_1NF_2-AF1#17 are presented in Figs. 3(c) and 3(d) and for samples #2 and #24 in Figs. 3(e) and 3(f), respectively. In Figs. 3(c), 3(e), and 3(f) the MR loops were recorded at temperatures fixed close to the middle of the SC transitions at $H = 0$ Oe, while in Fig. 3(d), $T_3 \approx 3.540$ K is close to the end of the transition. For temperatures in the middle of the SC transition, upward MR claws of large magnitude, reaching about 40% of the resistance at ± 4 kOe [see Fig. 3(c)], located close to the coercive fields of the $Cu_{41}Ni_{59}$ layer are observed for the samples with thinner CuNi layer (#17 and #24), whereas broad and flat cusps are found for sample #2 corresponding to the CR-APA range of fields of the loop in Fig. 2. At $T_3 \approx 3.540$ K, sample #17 passes through a sequence of resistive-SC-resistive transitions [see Fig. 3(d)] confined to the magnetic configurations in the system. Quantitative comparison of the MR, AMR, and $m(H)$ data for the thinner samples (#17 and #24) allows us to identify the spikes positions with the CR magnetic moment configurations of the Co and $Cu_{41}Ni_{59}$ layers.

Several reasons may generate the observed *R(T, H)* curves, reflecting the unconventional behavior of the SC transition temperature[24,25]: (1) a magnetic domain structure in the F layers, (2) Abrikosov vortices induced in the bottom SC Nb layer by the $Cu_{41}Ni_{59}$ alloy stray fields at perpendicular alignment of its magnetic moment, and (3) the triplet pairing generation in the spin-valve structure. We excluded the possibility of current-dependent quasiparticle accumulation in the NCA state[25,26] because no marked change in MR was observed for currents from 1 μA to 100 μA.

The mazelike domain structure, developed in $Cu_{47}Ni_{53}$ films below the saturation field, has a spatial period of about 100 nm (Ref. 21; Fig. 3), which is much larger than the coherence lengths in our system.[18] Thus, effects arising from Cooper pairs in which the electrons experience an inhomogeneous magnetic field can be neglected. Nevertheless, stray fields of the domain structure could have an influence on T_c, which may be constructive[27] or destructive.[28] The first case would lead to downward peaks in the $R(H)$ sweeps in the range of the SC transition, which we did not observe. The second case would yield upward peaks due to a reduction of T_c, which is strongest for the demagnetized state at the coercive field and vanishes for the single-domain state. A resistive peak arising from this effect is, however, expected to extend over the entire range of about ± 1 kOe, in which the hysteresis curve of the $Cu_{41}Ni_{59}$ alloy layer changes between the saturation values [see Fig. 2(b)], which is much wider than the peak structure observed in Fig. 3. Moreover, there should be present two structures of this type for every sweep, because the $Cu_{41}Ni_{59}$ and Co layers should both generate such a scenario.[29,30] In our experiments there is, however, only one resistance peak per sweep of the magnetic field. For specimens where the superconductor is sandwiched between two ferromagnets, pairs of domain walls coupled across the superconductor are proposed to generate a stray-field-induced resistance enhancement by multidomain states.[31] This can, however, not be a suitable mechanism in our $S/F_1/N/F_2/AF$ heterostructure with adjacent ferromagnetic layers.

On the other hand, although there is the nc-Nb/$Cu_{41}Ni_{59}$ interlayer between the Co and the SC Nb, there is an influence on the superconductor via the proximity effect.[32] This influence is clearly seen, as the T_c of the samples of the present work is reduced below that one of the specimens of comparable thickness of the Nb film in Ref. 18. The dependence on the thickness of the $Cu_{41}Ni_{59}$ layer in our spin-valve heterostructure, however, is weak compared to the overall suppression.

The stray field issue is closely related to the vortex-antivortex generation in the SC Nb film. Their motion would result in a transition temperature reduction.[33]

These scenarios were, moreover, checked with MR measurements of the pilot Nb/$Cu_{41}Ni_{59}$/Si-cap sample in the same geometry and at the midtransition temperature [see inset in Fig. 3(d)]. A similar influence of the $Cu_{41}Ni_{59}$ domain structure on superconductivity of the Nb layer, as in the Nb/$Cu_{41}Ni_{59}$/nc-Nb/Co/CoO_x structure, is expected.[34] However, no MR claws were observed in these pilot measurements, made for samples with the primary Nb layer thicker (not shown here) and thinner [inset in Fig. 3(d)] than $d_{Nb} \approx 12$ nm of our spin-valve series SF_1NF_2-AF1. This means that the stray fields, although being not generally negligible, do not generate the observed resistance peaks. Thus, scenarios (1) and (2) can be excluded.

The experimental findings can be consistently described in the framework of the existing theory of the $S/F_1/F_2$ core structure[17,35] [i.e., scenario (3)] The $S/F_1/F_2$ core, compared with the $F_1/S/F_2$ or $F_1/S/F_1$ cores design,[36–38] allows not only T_c for the PA (T_c^{P}) to be lower than for the APA (T_c^{AP}) of the F_1 and F_2 magnetic moments ($T_c^{P} < T_c^{AP}$—the "direct" spin-valve effect) but also the opposite ($T_c^{AP} < T_c^{P}$—the "inverse" spin-valve effect). Moreover, a nonmonotonic dependence of

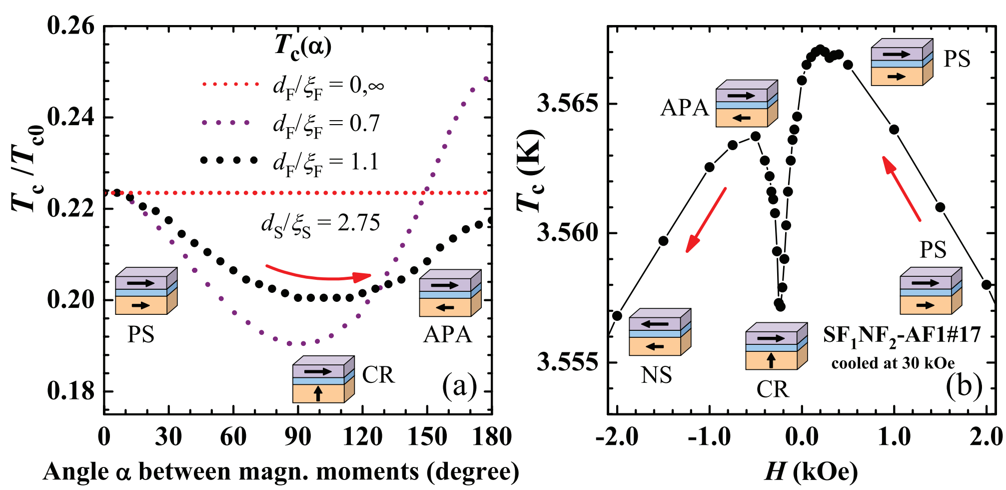

FIG. 4. (Color) (a) The angular dependence of the critical temperature T_c according to the model developed in Ref. 17. Here, T_{c0} is the critical temperature that the free-standing S-film would have. (b) Dependence of the critical temperature T_c on the magnetic field, swept along the hysteresis loop shown in Fig. 2. The direction of the field sweep in the panel (b) is shown by red arrows; the corresponding evolution of T_c in the panel (a) occurs along the red arrow. Physically, the NS state is not equal to the initial PS state because the magnetic anisotropy of the system is not uniaxial, but unidirectional (see Fig. 2). Here d_F, d_S, ξ_F, and ξ_S are the thicknesses and the coherence lengths[18] of the ferromagnet F_1 and the superconductor, respectively

the SC transition temperature T_c on the angle between the magnetic moments of the adjacent ferromagnetic layers, F_1 and F_2, and the "triplet" spin-valve effect was predicted,[17] at which T_c^{TR} for the NCA of magnetic moments is the absolute minimum T_c, because $T_c^{TR} < \{T_c^{AP}, T_c^{P}\}$. The "direct" and "inverse" spin-valve effects were demonstrated, e.g., in a CoO_x/Fe/Cu/Fe/In heterostructure.[25] Below we argue that we could observe the new, "triplet" spin-valve effect in the Nb/$Cu_{41}Ni_{59}$/nc-Nb/Co/CoO_x structure.

Two calculated curves, realizing all regimes mentioned above, are presented in Fig. 4(a). The predicted behavior can be compared with our experimental data in Fig. 4(b), where $T_c(H)$ taken at the midpoint of the resistive transition is presented. The data recording starts from the PS state at +4 kOe corresponding to the PS starting point of the MR measurements in Figs. 3(c) and 3(d). After the field polarity change, $T_c(H)$ rapidly drops and reaches the minimal T_c^{TR} at the field close to the negative coercive field [see Fig. 2(a)]. The downward spike in Fig. 4(b) coincides with the left (red) spikes in Figs. 3(c) and 3(d) and corresponds to the CR magnetic moments configuration of the $Cu_{41}Ni_{59}$ and the Co layers as indicated by the pictogram. We identify the T_c drop in Fig. 4(b) with the "triplet" spin-valve effect predicted in Ref. 17.

In the theory,[17] the two layers of weak ferromagnets are considered with a short electron mean-free path. The outer ferromagnetic layer is infinitely thick. Superconductivity in the heterostructure is treated using the Usadel equations.[39] This seems to be not applicable if one of the layers is made of a strong ferromagnet like cobalt. However, the functional layer adjacent to the Nb film is $Cu_{41}Ni_{59}$, a weak ferromagnetic alloy. Apart from suppressing T_c of the system independently of the thickness of the F_1 ($Cu_{41}Ni_{59}$) layer (see Fig. 4(a) for $\alpha = 0$), the outer ferromagnetic layer serves in the theory as a mixer of the singlet and triplet pairing channels for the adjacent functional layer. Since Co has a very short coherence length, ξ_F (Co) ≈ 1.3 nm,[40] d_{Co}/ξ_F (Co) ≈ 12 and 17 for $d_{Co} \approx 16$ nm and 22 nm, respectively (see caption of Fig. 1 for d_{Co}). Although there is a certain change of d_{Co} along the $Cu_{41}Ni_{59}$ wedge, the Co layer is always physically infinite as required by the theory.

IV. SUMMARY

In summary, we observed experimentally unusual MR peaks and sequences of resistive to SC and vice versa transitions in the Nb/$Cu_{41}Ni_{59}$/nc-Nb/Co/CoO_x spin-valve heterostructure associated with coercive fields of the $Cu_{41}Ni_{59}$ layer and attributed to a noncollinear magnetic configuration of the ferromagnetic layers in the structure. The SC transition temperature shift in a magnetic field and a careful analysis of magnetic configurations in the system allowed us to conclude that we observed experimentally the predicted novel triplet spin-valve effect.

ACKNOWLEDGMENTS

The authors are grateful to V. V. Ryazanov, A. D. Zaikin, and R. G. Deminov for stimulating discussions, to D. Vieweg for assistance in magnetic measurements, and to S. Heidemeyer, B. Knoblich, and W. Reiber for assistance in the TEM sample preparation. The work was supported by the Deutsche Forschungsgemeinschaft (DFG) Grant No. GZ: HO 955/6-1,2 and in part by the Russian Fund for Basic Research (RFBR) under Grants No. 11-02-00848-a (L.R.T.) and No. 12-02-90010-Bel_a (M.Yu.K.).

[1] F. S. Bergeret, A. F. Volkov, and K. B. Efetov, Phys. Rev. Lett. **86**, 4096 (2001).
[2] A. F. Volkov, F. S. Bergeret, and K. B. Efetov, Phys. Rev. Lett. **90**, 117006 (2003).
[3] F. S. Bergeret, A. F. Volkov, and K. B. Efetov, Rev. Mod. Phys. **77**, 1321 (2005).
[4] M. Eschrig, Phys. Today **64**, 43 (2011).
[5] R. S. Keizer, S. T. B. Goennenwein, T. M. Klapwijk, G. Miao, G. Xiao, and A. Gupta, Nature (London) **439**, 825 (2006).
[6] I. Sosnin, H. Cho, V. T. Petrashov, and A. F. Volkov, Phys. Rev. Lett. **96**, 157002 (2006).
[7] D. Sprungmann, K. Westerholt, H. Zabel, M. Weides, and H. Kohlstedt, Phys. Rev. B **82**, 060505(R) (2010).
[8] T. S. Khaire, M. A. Khasawneh, W. P. Pratt, Jr., and N. O. Birge, Phys. Rev. Lett. **104**, 137002 (2010).
[9] J. Wang, M. Singh, M. Tian, N. Kumar, B. Liu, Ch. Shi, J. K. Jain, N. Samarth, T. E. Mallouk, and M. H. W. Chan, Nat. Phys. **6**, 389 (2010).
[10] J. W. A. Robinson, J. D. S. Witt, and M. G. Blamire, Science **329**, 59 (2010).
[11] M. S. Anwar, F. Czeschka, M. Hesselberth, M. Porcu, and J. Aarts, Phys. Rev. B **82**, 100501(R) (2010).
[12] T. Yu. Karminskaya and M. Yu. Kupriyanov, Pis'ma Zh. Eksp. Teor. Fiz. **86**, 65 (2007) [JETP Lett. **86**, 61 (2007)].
[13] M. Houzet and A. I. Buzdin, Phys. Rev. B **76**, 060504(R) (2007).
[14] T. Yu. Karminskaya, M. Yu. Kupriyanov, and A. A. Golubov, Pis'ma Zh. Eksp. Teor. Fiz. **87**, 657 (2008) [JETP Lett. **87**, 570 (2008)].
[15] J. Zhu, I. N. Krivorotov, K. Halterman, and O. T. Valls, Phys. Rev. Lett. **105**, 207002 (2010).
[16] J. Y. Gu, J. Kusnadi, and C.-Y. You, Phys. Rev. B **81**, 214435 (2010).
[17] Ya. V. Fominov, A. A. Golubov, T. Yu. Karminskaya, M. Yu. Kupriyanov, R. G. Deminov, and L. R. Tagirov, Pis'ma Zh. Eksp. Teor. Fiz. **91**, 329 (2010) [JETP Lett. **91**, 308 (2010)].
[18] V. I. Zdravkov, J. Kehrle, G. Obermeier, S. Gsell, M. Schreck, C. Müller, H.-A. Krug von Nidda, J. Lindner, J. Moosburger-Will, E. Nold, R. Morari, V. V. Ryazanov, A. S. Sidorenko, S. Horn, R. Tidecks, and L. R. Tagirov, Phys. Rev. B **82**, 054517 (2010).
[19] V. Zdravkov, A. Sidorenko, G. Obermeier, S. Gsell, M. Schreck, C. Müller, S. Horn, R. Tidecks, and L. R. Tagirov, Phys. Rev. Lett. **97**, 057004 (2006).
[20] A. Ruotolo, C. Bell, C. W. Leung, and M. G. Blamire, J. Appl. Phys. **96**, 512 (2004).
[21] I. S. Veshchunov, V. A. Oboznov, A. N. Rossolenko, A. S. Prokofiev, L. Ya. Vinnikov, A. Yu. Rusanov, and D. V. Matveev, Pis'ma Zh. Eksp. Teor. Fiz. **88**, 873 (2008) [JETP Lett. **88**, 758 (2008)].
[22] F. Radu and H. Zabel, in *Magnetic Heterostructures*, edited by H. Zabel and S. D. Bader (Springer, Berlin, 2008), Vol. 227, Chap. 3, p. 97.
[23] A. L. Geiler, V. G. Harris, C. Vittoria, and N. X. Sun, J. Appl. Phys. **99**, 08B316 (2006).

[24] A. Yu. Rusanov, T. E. Golikova, and S. V. Egorov, Pis'ma Zh. Eksp. Teor. Fiz. **87**, 204 (2008) [JETP Lett. **87**, 175 (2008)].
[25] P. V. Leksin, N. N. Garif'yanov, I. A. Garifullin, J. Schumann, V. Kataev, O. G. Schmidt, and B. Büchner, Phys. Rev. Lett. **106**, 067005 (2011).
[26] A. Yu. Rusanov, S. Habraken, and J. Aarts, Phys. Rev. B **73**, 060505(R) (2006).
[27] T. Champel and M. Eschrig, Phys. Rev. B **71**, 220506(R) (2005).
[28] M. Lange, M. J. Van Bael, and V. V. Moshchalkov, Phys. Rev. B **68**, 174522 (2003).
[29] D. Stamopoulos, E. Manios, and M. Pissas, Supercond. Sci. Technol. **20**, 1205 (2007).
[30] A. K. Suszka, F. S. Bergeret, and A. Berger, Phys. Rev. B **85**, 024529 (2012).
[31] J. Zhu, X. Cheng, C. Boone, and I. N. Krivorotov, Phys. Rev. Lett. **103**, 027004 (2009).
[32] H. Yamazaki, N. Shannon, and H. Takagi, Phys. Rev. B **81**, 094503 (2010).
[33] I. S. Burmistrov and N. M. Chtchelkatchev, Phys. Rev. B **72**, 144520 (2005).
[34] R. Steiner and P. Ziemann, Phys. Rev. B **74**, 094504 (2006).
[35] S. Oh, D. Youm, and M. R. Beasley, Appl. Phys. Lett. **71**, 2376 (1997).
[36] L. R. Tagirov, Phys. Rev. Lett. **83**, 2058 (1999).
[37] Ya. V. Fominov, A. A. Golubov, and M. Yu. Kupriyanov, Pis'ma Zh. Eksp. Teor. Fiz. **77**, 609 (2003) [JETP Lett. **77**, 510 (2003)].
[38] J. Kehrle, V. I. Zdravkov, G. Obermeier, J. Garcia-Garcia, A. Ullrich, C. Müller, R. Morari, A. S. Sidorenko, S. Horn, L. R. Tagirov, and R. Tidecks, Ann. Phys. (Berlin) **524**, 37 (2012).
[39] K. D. Usadel, Phys. Rev. Lett. **25**, 507 (1970).
[40] Jun-Jih Liang, S. F. Lee, W. T. Shih, W. L. Chang, C. Yu, and Y. D. Yao, J. Appl. Phys. **92**, 2624 (2002).